ADVANCES IN INORGANIC CHEMISTRY, VOL. 40

STRUCTURE AND FUNCTION OF NITROGENASE

DOUGLAS C. REES, MICHAEL K. CHAN, and JONGSUN KIM

Division of Chemistry and Chemical Engineering, California Institute of Technology, Pasadena, California 91125

I. Introduction

As a constituent of nearly all biomolecules, nitrogen is essential for life. Although there is an enormous reservoir of molecular dinitrogen in the atmosphere, most organisms are unable to directly utilize this source due to the kinetic inertness of the dinitrogen molecule toward both oxidation and reduction (*1*). Fortunately, a group of prokaryotic organisms have acquired the ability to reduce dinitrogen to the metabolically usable form of ammonia and hence play an essential role in maintaining a stable level of nitrogen in the Earth's biosphere. The biochemical machinery required for this process of biological nitrogen fixation is provided by the nitrogenase enzyme system (*2–8*), which consists of two component proteins, the iron (Fe-) protein and the molyb-

denum-iron (MoFe-) protein. In the absence of molybdenum, alternate nitrogenase systems homologous to the molybdenum-containing "conventional" nitrogenase system may be induced (*9, 10*). Nitrogenase catalyzes not only the reduction of dinitrogen to ammonia, but also the reduction of protons to hydrogen (which appears to be an obligatory part of dinitrogen reduction) and the reduction of alternate substrates such as acetylene, azide, or cyanide. Substrate reduction by nitrogenase involves three basic types of electron transfer steps (Fig. 1): (i) the reduction of Fe-protein by electron carriers such as flavodoxin or ferredoxin; (ii) transfer of single electrons from Fe-protein to MoFe-protein in a MgATP dependent process, with a minimal stoichiometry of two molecules of MgATP hydrolyzed per electron transferred; and (iii) electron and proton donation to the substrate, which is almost certainly bound to the active site within the MoFe-protein. The overall reaction stoichiometry of the nitrogenase-catalyzed reaction has been established (*11*) as,

$$N_2 + 8H^+ + 8e^- + 16MgATP \longrightarrow 2NH_3 + H_2 + 16MgADP + 16P_i$$

where the release of protons associated with hydrolysis of MgATP has been neglected. The kinetics of dinitrogen reduction have been extensively studied (*12–14*) and show that nitrogenase is a relatively slow enzyme, with a turnover time per electron of ~5 sec^{-1}. Each electron transfer step between Fe-protein and MoFe-protein involves an obligatory cycle of association and dissociation of the protein complex, with the dissociation step having been identified as rate determining for the overall reaction. Considerable attention has been focused on the mechanistic details by which nitrogenase overcomes the kinetic barriers to dinitrogen reduction at ~1 atm pressure and room temperature, in contrast with present industrial processes that require both high temperatures and pressures. As a consequence of both the intrinsic biochemical and chemical significance of nitrogen fixation and the tech-

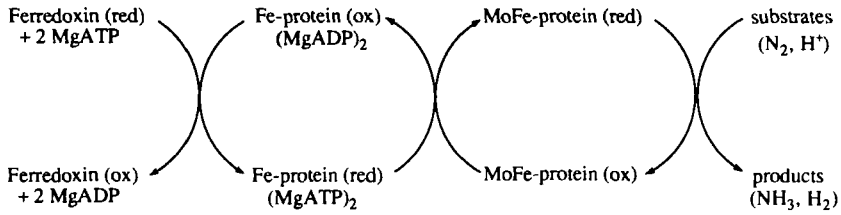

FIG. 1. Schematic reaction mechanism for substrate reduction by nitrogenase.

nological interest in the development of new catalysts for industrial ammonia synthesis, the properties and reaction mechanism of the nitrogenase proteins have been extensively probed.

The focus of this review will be primarily on the structures of the metal centers and polypeptide chains of the nitrogenase proteins, based on crystallographic structures of both the Fe-protein and the MoFe-protein, which have been recently determined at Caltech (*15–19*). Structural work on the MoFe-protein is also underway in the laboratory of J. Bolin at Purdue (*19a*). To minimize overlap with the existing, excellent reviews on the chemistry, biochemistry, biophysics, and genetics of nitrogenase and related chemical systems (*2–8*), these topics will be primarily discussed in the context of the nitrogenase protein structures.

II. Properties of the Nitrogenase Proteins

The two nitrogenase proteins, Fe-protein and MoFe-protein, are composed of a total of three different types of subunits and contain three different types of metal centers. The properties of the nitrogenase proteins have been extensively studied and are summarized below. To distinguish the two nitrogenase proteins isolated from different bacterial sources, the MoFe-protein and Fe-protein are designated as components "1" and "2," respectively, preceded by a two-letter abbreviation of the source species and genus; i.e., Av1 is MoFe-protein isolated from *Azotobacter vinelandii* and Cp2 is Fe-protein isolated from *Clostridium pasteurianum,* etc.

A. Nitrogenase Iron-Protein

The Fe-protein is a dimer of two identical subunits (coded by the *nifH* gene), with a total molecular weight of ~60,000. The amino acid sequences of over 20 different Fe-proteins have been determined and indicate that this protein is highly conserved in both the conventional and the alternate nitrogenases (*20*). For example, two of the more divergent Fe-protein sequences, from *A. vinelandii* (*21*) and *C. pasteurianum* (*22*), are 69% identical. The Fe-protein dimer contains one 4Fe:4S cluster, which is coordinated to each subunit through Cys-97 and Cys-132 (*23, 24*) (sequence numbering of the *A. vinelandii* Fe-protein is used throughout this paper). The reduced form of the cluster is EPR active, as observed for the 4Fe:4S clusters of ferredoxins. Unlike the cluster in ferredoxins, however, the 4Fe:4S cluster in Fe-protein exhib-

its a mixture of $S = \frac{3}{2}$ and $S = \frac{1}{2}$ spin states, with the equilibrium between the two states being solvent dependent (*25–28*). This solvent dependence suggests that the cluster environment is significantly more exposed in Fe-protein than in other 4Fe:4S clusters containing proteins, such as ferredoxins.

The Fe-protein dimer has two nucleotide binding sites for MgADP and/or MgATP, with dissociation constants of $\sim 100\ \mu M$, although considerable variations in measured binding constants have been reported (*29*). In the absence of MoFe-protein and reductant, Fe-protein exhibits no catalytic ATPase activity. Oxidized Fe-protein binds both nucleotides more tightly than does reduced Fe-protein, resulting in a decrease in the redox potential from -300 mV to -430 and -490 mV in the presence of MgATP and MgADP, respectively (*30*). Changes in the EPR spectra (*31*) and the ability of α,α-dipyridyl to chelate iron from the 4Fe:4S cluster (*32–36*) indicate that nucleotide binding is accompanied by changes in the Fe-protein structure. The cluster chelation behavior provides an especially convenient experimental approach to characterize Fe-protein–nucleotide interactions. In the absence of nucleotides, α,α-dipyridyl chelates iron slowly from Fe-protein. In the presence of MgATP, however, the iron is readily removed by this chelator, whereas in the presence of MgADP, iron chelation is inhibited. Furthermore, the chelation behavior depends on the oxidation state of Fe-protein (*35*). The sensitivity of iron chelation to the conformational, oxidation, and nucleotide binding states of Fe-protein provides a convenient probe for studying the coupling between nucleotide binding and cluster properties. For example, iron chelation studies have been very useful in characterizing site-directed mutants of Fe-protein in which the normal signal transduction mechanism between the nucleotide binding site and the cluster has been disrupted (*37–39*).

In addition to the mechanistic role in the nitrogenase enzymatic function, Fe-protein also participates at several stages in the biosynthesis of the nitrogenase proteins. Fe-protein is essential for the production of active MoFe-protein and is involved in both the synthesis of FeMo-cofactor and its insertion into cofactor-deficient MoFe-protein (*40–42*). Fe-protein may also function as an activator for the expression of alternative nitrogenases (*43*). In turn, formation of active Fe-protein requires the *nifM* gene product (*44, 45*), which perhaps functions either in cluster insertion or in promoting the correct subunit–subunit and subunit–cofactor interactions in the Fe-protein dimer (i.e., a chaperone-type role). The significant sequence conservation observed in the Fe-protein family may reflect the structural constraints associated with these diverse aspects of Fe-protein function.

B. Nitrogenase Molybdenum-Iron Protein

The MoFe-protein is an $\alpha_2\beta_2$ tetramer (with the subunits coded by the *nifD* and *nifK* genes, respectively), with a total molecular weight of ~240,000. The two subunits are of similar size; for example, the isolated α and β subunits of *A. vinelandii* MoFe-protein have 491 and 522 amino acids, respectively (*46*). In general, the amino acid sequences of MoFe-proteins are less well conserved than are Fe-protein sequences, so that the MoFe-protein sequences from *A. vinelandii* and *C. pasteurianum* are only 36% identical (*47*). Associated with the MoFe-protein tetramer are approximately 2 molybdenum atoms, 30 iron atoms, and 30 sulfur atoms that are organized into two types of metal centers: the FeMo-cofactor and the P-cluster pair. The structures and properties of these centers have been extensively probed by a wide variety of techniques.

1. FeMo-Cofactor

The FeMo-cofactor (*48, 49*), also referred to as the M-center, was first identified by Shah and Brill (*50*) as a stable metallocluster isolated from acid-denatured MoFe-protein. Isolated cofactor can fully activate a defective MoFe-protein obtained from the mutant *A. vinelandii* strain UW45, which contains P-cluster pairs, but not the EPR active ($S = \frac{3}{2}$) center that is characteristic of nitrogenase. Intense interest has been focused on the FeMo-cofactor since it contains molybdenum in a biologically unprecedented form and is believed to represent the site of substrate reduction (*51, 52*), although isolated cofactor exhibits no catalytic activities. The FeMo-cofactor has a composition of one Mo atom, seven Fe atoms, eight to nine inorganic sulfurs, and one homocitrate group (*16, 48, 49, 53–55*). The redox properties and oxidation states of the cofactor are intimately associated with the ability of this center to function in substrate reduction. Three oxidation states differing by one electron, M(r), M(s-r), and M(ox), appear to be accessible to the FeMo-cofactor within the MoFe-protein (Fig. 2) (*49*). M(s-r) is the semireduced form of the FeMo-cofactor that is normally isolated in the presence of excess dithionite and is characterized by a unique $S = \frac{3}{2}$ EPR signal. M(s-r) may be oxidized by one-electron at a potential of ~ -50 mV to give the M(ox) state. A one-electron reduced form of the cofactor, M(r), is produced only under turnover conditions, at a potential estimated at ~ -470 mV. Both the M(ox) and the M(red) states are EPR silent. The net oxidation states of the metals in the complex are not known. The Mo may formally exhibit the +4 oxidation state, whereas Mössbauer studies suggest that the average oxidation state of Fe is +2.67. The

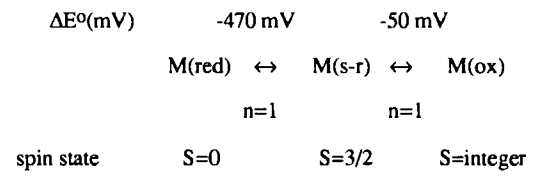

FIG. 2. Oxidation-reduction properties of the FeMo-cofactor. M(ox), M(s-r), and M(r) represent the oxidized, semireduced (dithionite isolated form), and reduced form, respectively, of the protein-bound FeMo-cofactor (*49*).

isolated cofactor has a net negative charge, however, which, if this reflects the charge on the core of the protein-bound cluster, would indicate that, formally, the Fe must be primarily in the ferrous (+2) state. A satisfactory description of the electronic and oxidation properties of the FeMo-cofactor remains an important problem.

2. P-Cluster Pair

The P-cluster pair (*56*) may function in the transfer of electrons between the Fe-protein and FeMo-cofactor. Mössbauer, EPR, and extrusion studies indicated that the P-cluster pair contained 4Fe:4S-type clusters (*57–62*) that are in close proximity (*63–65*), which was also suggested from an analysis of anomalous scattering effects from Cp1 (*66*). These studies also demonstrate, however, that the detailed properties of this center are distinct from better characterized proteins that contain one or more mononuclear 4Fe:4S clusters. Mössbauer studies indicated that the iron atoms in each center could be assigned to three distinct types, designated D, Fe^{+2}, and S, in the approximate ratio 5:2:1. These sites could be grouped into pairs with compositions (D_3Fe^{+2} and D_2SFe^{+2}) that have slightly different spectroscopic properties. The isomer shifts are consistent with all iron sites in the dithionite reduced form of the P-cluster pair formally having the ferrous oxidation state, which is unprecedented in biological 4Fe:4S systems. Redox titrations of the P-cluster pair have identified the oxidation states P^N, P^{OX1}, P^{OX2}, and higher oxidation states (Fig. 3) (*65*). P^N denotes the P-cluster pair state observed in dithionite reduced MoFe-protein. The oxidation of P^N to P^{OX} has been described as an $n = 2$ process, although evidence for intermediates generated by $n = 1$ steps has been presented (*67*). More reduced forms of the P-cluster pair have not been described, although it is possible that they could be produced, perhaps transiently, under turnover conditions.

Although not as extensively studied as the Fe-protein, adenosine nucleotides, particularly MgADP, can also bind to the MoFe-protein

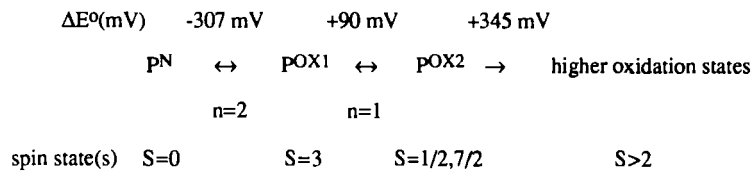

FIG. 3. Oxidation-reduction properties of the P-cluster pair. P^N represents the form of the P-cluster pair found in dithionite isolated MoFe-protein, whereas P^{OX} represents more oxidized forms of the center (*65*).

(*68*). Recent EPR and ENDOR studies on the binding of manganese substituted adenosine nucleotides have been interpreted to suggest that these nucleotides may bind near the P-cluster pair (*69*).

III. Structural Description of the Nitrogenase Proteins

A. Crystal Structure Determinations

Because descriptions of the structure determinations for Fe-protein and MoFe-protein have been published (*15–19*), only general features will be presented here. An essential component to the success of the structure determinations was the availability of multiple crystal forms for both Fe-protein and MoFe-protein. Nitrogenase proteins isolated from both *A. vinelandii* and *C. pasteurianum* (Av1, Av2, Cp1, and Cp2) were used for this purpose. Presumably due to the sensitivity of the nitrogenase metal centers to oxygen and oxidants, preparation of suitable heavy atom derivatives was problematic since most transition metal complexes used for derivatives tend to be oxidants. Heavy atom derivatives of moderate quality were finally prepared for both the Fe-protein, using the antiarthritic drug myochrisine (gold sodium thiomalate), which binds to the 4Fe:4S cluster, and the MoFe-protein, using ethylmercurithiosalicylate, which binds to cysteines, and the platinum compounds $K_2[PtCl_4]$ and di-μ-iodobis{(ethylenediamine)-di-platinum-(II)} nitrate, which bind to methionines. However, electron density maps phased from these derivatives did not permit the complete tracing of the polypeptide chain. To improve the quality of these maps, the electron density maps were averaged within and between multiple crystal forms. The utility of multiple crystal forms can be appreciated since, in effect, each additional crystal form is approximately equivalent in terms of phasing information to a new heavy atom derivative. Models were built into these maps, refined, and used to calculate im-

proved electron density maps in an iterative process until essentially complete models were obtained. At present, the Av1, Cp1, and Av2 structures have been refined at resolutions of 2.2, 3.0, and 2.9 Å, respectively, with R factors ≤ 0.20 and good geometry. The use of multiple crystal forms to improve maps is not a new idea (e.g., *70*), but this method should become increasingly valuable in the crystallographic analysis of larger proteins, where accurate experimental phases are more difficult to obtain.

At the initial resolution of the MoFe-protein structure analysis (2.7 Å), it was not possible to unambiguously establish the detailed geometry and chemical identities of all the constituents of novel metal centers such as the FeMo-cofactor and P-cluster pair. Consequently, models for these centers were built into electron density maps using fragments of well-characterized clusters as the basic building blocks (*71, 72*). This process was rather like the use of amino acid fragments to fit electron density maps of proteins of unknown sequence. The redox centers were identified as the strongest features in the electron density map and were consistent with the highest peaks in both native anomalous difference Patterson and Fourier maps. As native anomalous scattering effects were not used in the phasing of the MoFe-protein structure, the initial electron density maps were not influenced by any specific model for the centers. The FeMo-cofactor and P-cluster pair were identified from the positions of amino acid residues that had been identified from mutagenesis studies as components of the cofactor environment, including residues α275 and α195 for FeMo-cofactor and residues α62, α88, α154, β70, β95, and β153 for the P-cluster pair (*73–79*). At 2.7 Å resolution, atoms are not resolved, so that the identities of the various sites were inferred from the available analytical and spectroscopic information.

The structural details of the metal centers in the MoFe-protein that were proposed based on the 2.7-Å-resolution diffraction analysis (*16, 17*) have been confirmed by more recent studies at 2.2 Å resolution (*18*). Despite the increased resolution, there are certain limitations to the structural description of the metal centers that can be achieved from crystallographic studies. As discussed in Howard and Rees (*80*), the unambiguous identification of individual atoms, including the possible presence of hydrides, and a more detailed description of the geometry and oxidation states will be extremely difficult, if not impossible, to establish solely on the basis of a macromolecular crystallographic study. This situation again emphasizes the necessity of complementary, interdisciplinary approaches in the investigation of complex biological phenomena.

B. Nitrogenase Iron-Protein Structure

The quarternary structure arrangement of the Fe-protein (*15*) consists of two subunits, each folded as a single α/β-type domain and connected at one surface by the 4Fe:4S cluster (Fig. 4) (*81*). At the core of each subunit is an eight-stranded β sheet (with seven of the eight β strands oriented in parallel fashion) flanked by nine α helices. Each subunit contains a characteristic structural motif near the amino terminus (residues 9–16) that is found in a major class of mononucleotide binding proteins (*82, 83*). The possible involvement of this region of Fe-protein in nucleotide binding was first recognized by sequence analysis (*84*). The two nucleotide binding sites in Fe-protein are located in the cleft formed between the two subunits. Consistent with a role for this region in nucleotide binding, molybdate ions from the crystallization solution are bound at positions that correspond to the location of the terminal nucleotide phosphate groups in other nucleotide binding proteins. Presumably, the molybdate is serving as a phosphate analogue in this situation. Each molybdate site is located ~20 Å from the cluster and ~20 Å from the symmetry-related molybdate site. This distance for the cluster–molybdate separation suggests that MgATP does not bind directly to the cluster, consistent with the conclusions from spectroscopic studies of this interaction (*85*).

A more detailed analysis of the crystal structure identified a nucleotide, modeled as ADP, that was bound to only one of the two nucleotide binding sites present in the dimer. The occupancy of this ADP has been estimated as ~0.4. Since the two potential nucleotide binding sites are not related by crystallographic symmetry, both sites need not be equally occupied. The nucleotide interacts with residues from both subunits: the terminal phosphate groups interact with residues 9–16, whereas the nucleotide ring contacts Tyr 159, Ala 160, Asn 163, and the main-chain atoms of 128–130 of the neighboring subunit. The ribose spans the subunit cleft and interacts with residues Lys 41 and Asp 129 from the different subunits. This nucleotide copurified with Av2 and may represent a tightly bound species of the type identified by Lindahl et al. (*86*). Additionally, Watt *et al.* (*30*) noted that up to seven ATP molecules could irreversibly bind to oxidized Av2 in the absence of Mg^{2+}. Consequently, the presence of a bound nucleotide in Av2 was not unexpected, although the functional significance of this group, if any, is unclear.

Since the phosphate groups of the nucleotide and the cluster are too distant (~20 Å) to permit direct chemical coupling of electron transfer and ATP hydrolysis, the location of both sites at the subunit interface

suggests that the interface provides the coupling mechanism. The simplest picture envisions two (or more) conformational states of Fe-protein that differ in the details of intersubunit interactions, with the equilibrium between the two states sensitive to the oxidation state of the cluster and nucleotide binding. This allosteric model for Fe-protein function naturally directs attention to interactions that might stabilize alternate quaternary structure arrangements of the subunits, such as salt bridges. A set of intersubunit salt bridges in Fe-protein that may function in this capacity are the cyclic arrangement of Asp 129 and Lys 41 in alternating fashion from both subunits, organized about the dimer twofold axis. Since both Lys 41 and Asp 129 interact with the bound nucleotide, this observation indicates that the Asp 129–Lys 41 and their respective interactions with the nucleotide could be mutually exclusive, thereby providing a mechanism for coupling the conformational state of the protein with nucleotide binding.

Many of these features of Fe-protein function may be relevant to nonnitrogenase biochemical systems. Striking sequence similarities have been noted in the cluster ligand, nucleotide binding, and interface regions between Fe-protein and the enzyme protobacteriochlorophyllide reductase, which catalyzes the first committed step in photosynthetic growth (*87, 88*). There are also general similarities between Fe-protein and other nucleotide binding proteins such as ras p21 and recA proteins. These proteins belong to a general family in which nucleotides stabilize alternate conformations of a protein, with binding to other macromolecules serving to induce a conformational switch for nucleotide hydrolysis that interconverts the two forms. One class of these proteins includes membrane-associated transporters, in which ATP hydrolysis is coupled to substrate translocation across a membrane. Many of these transporters, such as the ArsA protein functioning in arsenate transport (*89*), contain two nucleotide-binding domains. Based on the Fe-protein structure, it is plausible that the nucleotide binding sites are positioned at the interface between domains, permitting nucleotide-mediated changes in the domain positions to be directly transmitted to the translocation site. Allosteric switching between alternate conformational states of proteins, driven by nucleotide binding and hydrolysis, appears to provide a very general transducing mechanism for coupling the energy of nucleotide hydrolysis to a variety of biochemical processes.

C. Nitrogenase Molybdenum-Iron Protein Structure

The α and β subunits of the MoFe-protein exhibit similar polypeptide folds, consisting of three domains of the α/β type with some extra

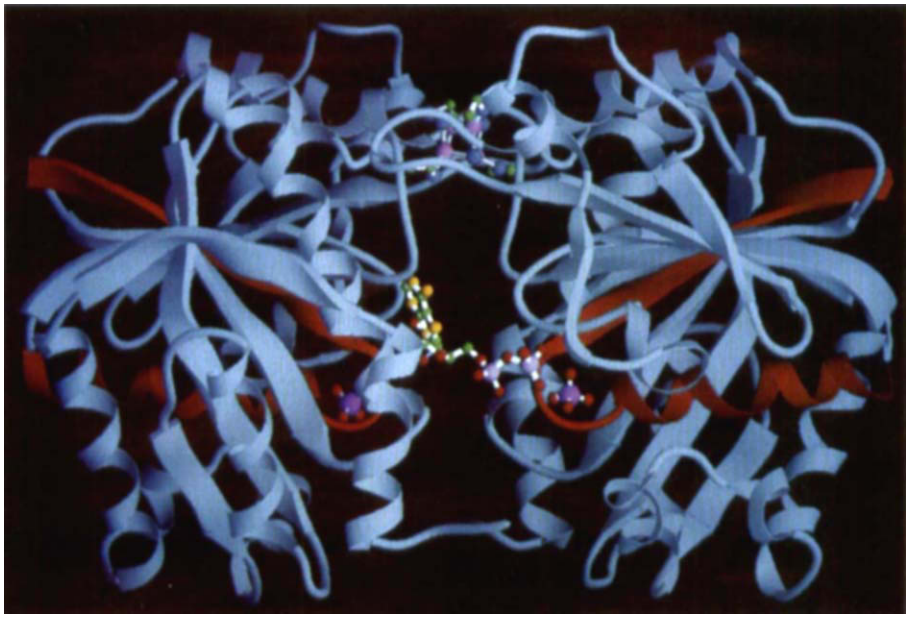

FIG. 4. Ribbon diagram (*81*) of the polypeptide chain fold of the *A. vinelandii* Fe protein (*15*). The nucleotide binding sequence at the amino terminus of Fe protein is red. The 4Fe:4S cluster, ADP, and molybdate are represented by atomic models.

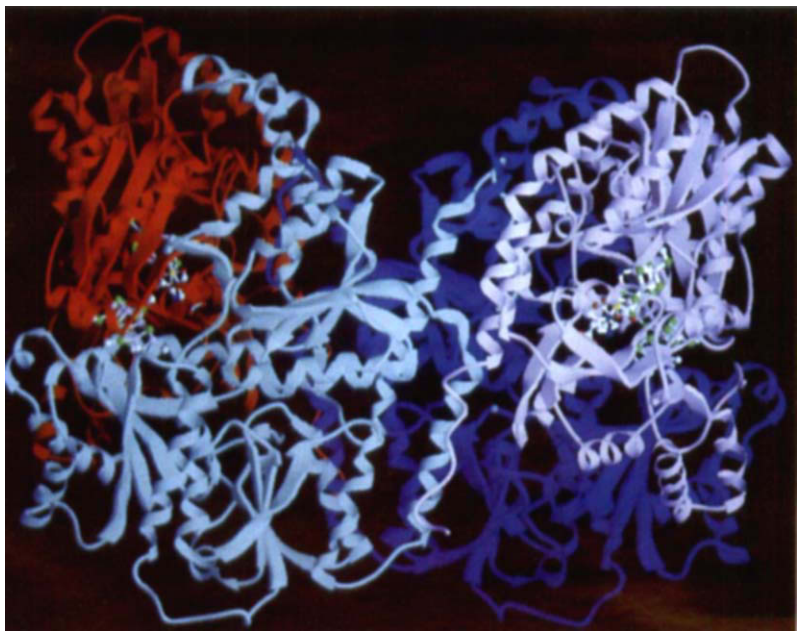

FIG. 5. Ribbon diagram (*81*) of the polypeptide chain fold of the *A. vinelandii* MoFe protein (*17*). The two α subunits in the MoFe-protein tetramer are colored red and lavender, while the two β subunits are colored dark blue and light blue. The FeMo cofactor and P-cluster pair are represented by atomic models.

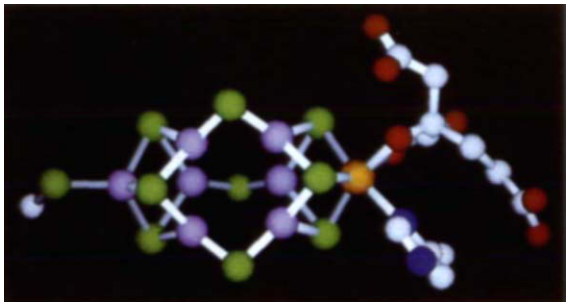

FIG. 6a. A ball-and-stick model (81) of the FeMo-cofactor.

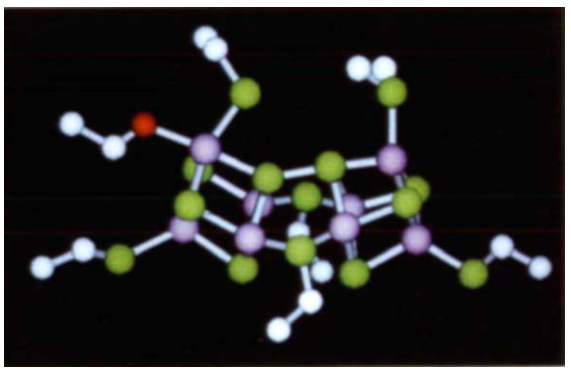

FIG. 7a. A ball-and-stick model (81) of the P-cluster pair.

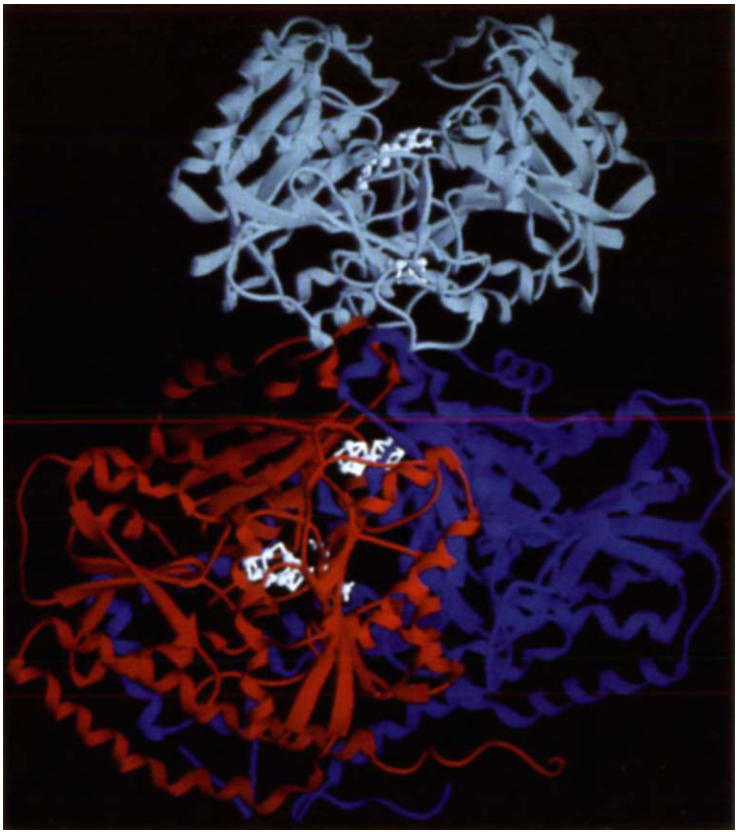

FIG. 8. Ribbon diagram (*81*) of a hypothetical model for the docking of Fe protein to an $\alpha\beta$ dimer of the MoFe protein. The Fe protein subunits, α subunit and β subunit, are colored light blue, red, and dark blue, respectively, while white atomic models are provided for the metal centers and ADP.

helices (Fig. 5) (*16*). Similarities between the N-termini of the α and β subunits were originally recognized in sequence analyses (*90*). Although the α/β-type fold is a common motif in protein structure, no significant homology to other proteins has been identified for the α- and/or β subunits from sequence comparisons, with the exceptions of the corresponding proteins in alternate nitrogenases and the protein products of the *nifE* and *nifN* genes. At the domain level, folding patterns similar to those of other proteins may be recognized; for example, D. Blow (personal communication) has noted that the folding pattern of the third domain of the α and β subunits is very similar to that found in the mononucleotide binding domain of tyrosyl-tRNA synthetase (*91*). In each subunit, there is a wide, shallow cleft among the three domains; in the α subunit, the FeMo-cofactor occupies the bottom of this cleft. The location for the FeMo-cofactor at the boundary among three domains is reminiscent of the site for the iron–sulfur cluster in aconitase (*92*). The site in the β subunit corresponding to the location of the FeMo-cofactor in the α subunit contains the side chains of residues His β193, Gln β294, His β297, and Asp β372. Interestingly, if the mononucleotide binding domain of tyrosyl-tRNA synthetase is superimposed onto the third domain of the β subunit, the location of nucleotide binding in the former structure occurs near these side chains. This raises the intriguing suggestion that perhaps the FeMo-cofactor binding site in the α subunit, and a nucleotide binding site in the β subunit, arose from homologous regions of these subunits. Crystallographic studies of nucleotide binding to MoFe-protein have not yet revealed any binding to this site, however.

Although there are no permanent channels leading from the surface to the FeMo-cofactor, it is possible that transient openings could be created among the α subunit domains that allow cluster insertion, substrate access, and product egress. Extensive contacts occur between the α and the β subunits in an $\alpha\beta$ dimer; this is especially evident by the bridging of the two subunits through the P-cluster pair. The α and β subunits within an $\alpha\beta$ dimer are approximately related by a twofold axis that passes through the P-cluster pair. The quaternary structure of the MoFe-protein may be considered to consist of a pair of $\alpha\beta$ dimers, where each $\alpha\beta$ dimer is related to the other by the intratetramer twofold axis. Although the α and β subunits in an $\alpha\beta$ dimer are also approximately related by a twofold rotation, the MoFe-protein does not exhibit 222 symmetry. Packing between helices from the β subunits dominate the interactions at the tetramer interface, with some contributions from helices in the α subunit. Interestingly, the center of the six α-helical barrel that surrounds the tetramer twofold axis is not filled with sidechains; rather, an open channel of ~8–10 Å in diameter and

~35 Å long could conceivably serve as a conduit for substrates and products to access the active sites. A calcium binding site coordinated between the two β subunits also appears to contribute to tetramer stabilization.

IV. Structures of the Metal Centers of Nitrogenase

A. 4Fe:4S Cluster of Iron-Protein

The 4Fe:4S cluster covalently links the two subunits. As had been predicted from chemical modification, genetic, and spectroscopic studies (*23, 24, 93*), the 4Fe:4S cluster is symmetrically coordinated to two cysteines, 97 and 132, from each subunit. Coordination of metal centers by residues from different subunits has been observed in the photosynthetic reaction center (*94, 95*), nitrite reductase (*96*), and the Mo-Fe protein (*16*), and may be a common feature of multisubunit metalloproteins. A striking feature of Fe-protein is the solvent exposure of the 4Fe:4S cluster, which had been recognized in spectroscopic studies (*25–28, 97*). This solvent exposure may contribute to the considerable sensitivity of Fe-protein to inactivation by oxygen. Other than the ligating cysteines, the only side chains that contact the cluster are Ala-98 from each subunit; in addition, the side chains of Val-130 and Phe-135 approach to within 5–6 Å of the cluster. Both cluster ligands are located near the N-terminal end of α helices that are directed toward the cluster, permitting favorable electrostatic interactions between the terminal amide groups of the helix and those of the anionic cluster. These favorable interactions are reflected in six potential NH—S hydrogen bonds (*98*), three from each subunit, that occur between sulfur atoms in the cluster and the NH groups of residues 98 and 134, and between the S_γ of residue 97 and the NH group of residue 99. The general impression of this region of the Fe-protein is of an exposed, loosely packed cluster environment that could be designed to function as a hinge or pivot that accommodates multiple conformations during the nitrogenase reaction.

B. FeMo-Cofactor

The FeMo-cofactor consists of two clusters of composition 4Fe:3S and 1Mo:3Fe:3S that are bridged by three nonprotein ligands (Fig. 6) (*16*). Compounds containing the 4Fe:3S cluster have been described (*99, 100*), although the terminal ligation of the Fe sites in these molecules

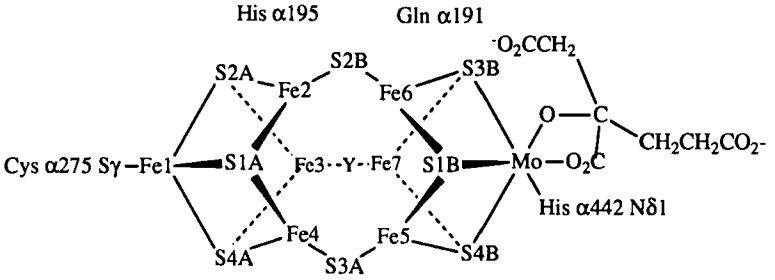

FIG. 6b. Schematic model of the FeMo-cofactor.

differs significantly from that observed in the FeMo-cofactor. Based on the electron density values at the positions of the bridging ligands, two of these ligands are assigned as sulfur (presumably S^{2-}), whereas the third ligand has ~20% lower electron density in the electron density maps calculated at 2.2 Å resolution for Av1 (*18*). This third bridging ligand, designated "Y," is most likely a less-well-ordered sulfur, although it might also be a well-ordered O/N species or even a disordered chloride. It is also possible that there could be compositional heterogeneity at this position, perhaps due to the presence of inactive protein, that is influencing the electron density in this region. Homocitrate, which is an essential component of FeMo-cofactor (*54, 55*), coordinates the Mo through a hydroxyl and carboxyl oxygen. There is no evidence in the electron density maps for a hexacoordinate sulfur atom at the center of the cluster. Consequently, a cavity appears inside the cofactor between the two cluster fragments. The longest metal–metal distance in the FeMo-cofactor is ~7.4 Å between sites Fe1 and Mo. The Fe—Fe separation distance between bridged iron sites (such as Fe2 and Fe6) is ~2.5 Å, whereas the distance between nonbridged iron sites on different cluster fragments (such as Fe2 to Fe5, etc.) is ~3.8 Å. The distance between Mo and the three closest irons of the 4Fe:3S fragment averages ~5.2 Å, which is approximately the same as the distance between Fe1 and the three irons of the 1Mo:3Fe:3S fragment.

If the threefold axes of the isolated 4Fe:3S and 1Mo:3Fe:3S clusters are superimposed, then the cluster is liganded to the protein through the metals (Fe1 and Mo) located on the threefold axis. The protein environment around the FeMo-cofactor is primarily provided by the α subunit. Cysteine α275 coordinates Fe1, whereas the Mo is liganded by the side chain of His α442. Site-directed mutagenesis studies had implicated Cys α275 as a cofactor ligand (*73, 74, 76*). Based on sequencing of Nif^- mutants altered in the α subunit, Zamir had proposed that

His α442 could coordinate the FeMo-cofactor (*101*). The side chains of two other residues proposed to be near the cofactor, His α195 (*75, 78, 79*) and Gln α191 (*102*), are within 4 Å of Fe2 and Fe6, respectively, but these residues are not directly liganded to the metals. Site-directed substitution of His α195 results in the loss of a nitrogen ESEEM signal from the MoFe-protein (*79*), which may originate from the coupling of that residue to the $S = \frac{3}{2}$ spin system of the cofactor through a side-chain hydrogen bond to one of the bridging sulfurs. The side chain of Gln α191 interacts with one of the carboxyl groups of homocitrate, which is consistent with a proposal based on site-directed mutagenesis studies (*102*). Cys α275, His α442, His α195, and Gln α191 are conserved in all known MoFe-protein sequences.

The tetrahedral coordination geometry of Fe1 and the octahedral coordination geometry for Mo are typical of the coordination environments for these metals observed in model compounds and Fe:S proteins (*4, 56, 71, 72*). An unusual feature of the FeMo-cofactor model, however, is the trigonal ligand geometry of the six Fe sites that bind the bridging sulfurs. Trigonal coordination geometry for Fe is not unprecedented, however, and has been described in a small molecule structure of an iron-thiolate species (*103*). In this case, the coordinating thiols contained bulky substituents, and it was proposed that the low coordination number of the Fe atoms reflected the effects of steric crowding between the ligands. No such corresponding features in the FeMo-cofactor environment are evident, however. Solvent molecules that might possibly serve as fourth ligands have not been observed. It is also unlikely, although not impossible, that a less electron dense group (such as O or N) could be present in the cluster interior. The separation distance of ~2.5 Å between bridged irons suggests that there might be some Fe—Fe bonding that could serve as a fourth coordination interaction.

The structural features of the FeMo-cofactor model are generally consistent with the results of analytical and spectroscopic (EXAFS, ENDOR, and Mössbauer) studies of the cofactor. The composition of the nonprotein part of the FeMo-cofactor model, 1Mo:7Fe:9S:1 homocitrate, is within the range of values that have been reported (*48, 53–55*). The absence of protein-bound bridging ligands between the two clusters in FeMo-cofactor is consistent with the ability to extract the intact cofactor from MoFe-protein. EXAFS studies of the Mo environment in both the MoFe-protein and the isolated cofactor indicate that 2–3O(N) and 3–5S are directly coordinated to Mo, with 3–4Fe present in the second coordination shell of Mo (*104, 105*); the crystallographic model contains 3O(N), 3S, and 3Fe. Studies of Fe EXAFS

on the isolated cofactor (*106*) indicate that, on average, each Fe is surrounded by ~3S and 0.3–0.8Mo (~2.7 Å), with ~ 2.2 and ~1.3 Fe atoms located at ~2.7 and ~3.8 Å, respectively. Assuming Y is a sulfur, the *average* Fe environment in the present FeMo-cofactor model bound to the MoFe-protein contains ~3.1S and ~0.4Mo, with ~3.4 and ~0.9 Fe atoms at ~2.7 and ~3.8 Å, respectively. Fe^{57} ENDOR studies (*107*) have indicated that five magnetically inequivalent iron species are present; neglecting the asymmetric protein environment and the chiral homocitrate ligand and assuming that the Y ligand is distinct from the other two bridging ligands, five different types of Fe sites are observed in the structural model (Fe1; Fe3; Fe7; Fe2 and Fe6; and Fe4 and Fe5). Mössbauer studies (*59, 60*) identified 5–7 iron sites in the FeMo-cofactor that could be grouped into two sets; however, assignment of these sites to particular atoms in the FeMo-cofactor model cannot be made at present.

The FeMo-cofactor is buried at least 10 Å below the protein surface in an environment primarily formed by the α subunit. Cys α275 and His α442, as well as Ser α278, which is hydrogen bonded to the S_γ of Cys α275, are strictly conserved in all known MoFe-protein sequences. Other highly conserved residues in the vicinity of the FeMo-cofactor include: Gly α356 and α357, which are required to avoid steric interference with the cofactor and whose NH groups form NH—S hydrogen bonds to one of the bridging sulfurs; Arg α96 and Arg α359, which can form hydrogen bonds to the Y ligand and a cluster S and which may serve to stabilize the FeMo-cofactor and/or partially reduced intermediates formed during substrate reduction; His α195, which hydrogen bonds to the third bridging ligand and may function in proton transfer reactions; and three residues, Gln α191, Glu α440, and Glu α427, which are near the homocitrate and interact with this group either directly or through water molecules. The protein environment around the FeMo-cofactor is primarily provided by hydrophilic residues, although there are some hydrophobic residues. The positioning of the FeMo-cofactor near the N-terminal ends of helices α280–α290 and α359–α369 may serve to stabilize the cluster electrostatically (*98*).

C. P-Cluster Pair

The P-cluster pair is formed by two 4Fe:4S clusters that are bridged by two cysteine thiol ligands (residues α88 and β95), which are further connected by a disulfide bond between two of the cluster sulfurs (Fig. 7) (*16–18*). The disulfide bond is particularly intriguing and it is located on the side of the P-cluster pair closest to the proposed (*17*) binding

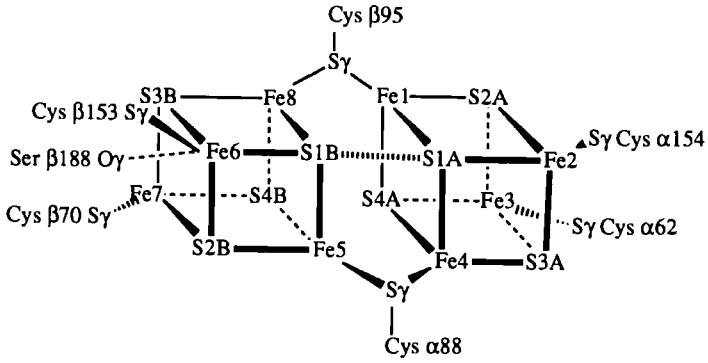

FIG. 7b. Schematic model of the P-cluster pair.

site for Fe-protein. To our knowledge this is the first example of a cluster containing a $(\mu_3\text{-S})_2$ disulfide, although an intermolecular disulfide bridged Fe_2S_2 cluster has been synthesized previously (*108*). Singly coordinating cysteine thiols (from residues α62, α154, β70, and β153) ligate the remaining four irons, such that nonbridging cysteines coordinated to a specific 4Fe:4S cluster are from the same subunit. In addition to the cysteine ligands, Ser β188 appears to coordinate Fe6 along with Cys β153. The coordination environments of both Fe6 and Fe2 are distorted from ideal tetrahedral geometry, due to interactions with Ser β188 and the main chain of Gly α185, respectively. The variety of different coordination environments for P-cluster pair irons is consistent with observations from Mössbauer spectroscopy for multiple classes of iron in this center, but no definitive correspondence between the structural and the spectroscopic categories can be made at present. The cysteine ligands to the P-cluster pair had been correctly identified from mutagenesis experiments (*73, 74, 76, 77*). Individual replacement of any of the six cysteines by alanine eliminates diazotropic growth of the mutant strains. Some non-alanine substitutions for Cys α88 and β153 have been described that can still produce nitrogenase with low activity, however, possibly as a consequence of the substituted residue functioning as a cluster ligand, through a structural rearrangement that allows a previously non-liganding group to coordinate the cluster, or simply because no ligand is actually needed. Additionally, substitution of Gly α185 with Asp has been found in a Nif^- mutant of nitrogenase (*101*).

As had been proposed from sequence comparisons and mutagenesis experiments (*73, 74, 76*), the P-cluster pair is located at the interface between the α and the β subunits. The approximate twofold symmetry

of the P-cluster pair is reflected in the sequence similarities between the polypeptide chain for the α subunit and that for the β subunit in this region (*90*). The P-cluster pair is buried ~12 Å below the surface in a protein environment that is mainly provided by hydrophobic residues. The location of the P-cluster pair near the N-terminal ends of six helices (α63–α74; α88–α92; α155–α159, β71–β81; β93–β106, and β153–β158) may serve to provide an electrostatic contribution to cluster stability (*98*). With the exception of the cluster ligands and Gln β93 and Thr β152, hydrophilic residues around the P-cluster pair, such as Glu α153, Glu α184, Ser α92, Ser α152, and Ser β92, are generally not conserved in different MoFe-protein sequences. The side chains of residues Cys α62, Cys α88, Cys α154, Cys β70, Cys β95, Cys β153, and Ser β188 are coordinated to the P-cluster pair and are strictly conserved. Strictly conserved Gly residues (α87, β94, and α185) around the P-cluster pair are also structurally important to avoid steric interference with metal clusters.

V. Mechanistic Features

The electron transfer steps that take place between the Fe-protein and the substrate bound to the MoFe-protein are not well understood. Basic questions concerning (1) the role of adenosine nucleotides in the nitrogenase mechanism; (2) whether the P-cluster pair serves as an intermediate electron carrier between Fe-protein and FeMo-cofactor, and (3) the sequence and number of electrons and protons transferred to the substrate and (possibly) intermediates are unanswered. Although the structures of the nitrogenase proteins cannot answer these questions, they do provide a basis for formulating mechanistic proposals that may be useful in attacking these problems. The following discussion is, of necessity, speculative and approaches the nitrogenase mechanism from the viewpoint of an electron traveling through the system; i.e., the sequence of steps is considered in the order Fe-protein to MoFe protein; P-cluster pair to FeMo-cofactor; and substrate binding and reduction at the FeMo-cofactor.

A. Interactions between MoFe-Protein and Fe-Protein

With the availability of the crystal structures for both nitrogenase proteins, some general features of the complex between the two proteins may be addressed. Two residues of Fe-protein that have been identified as interacting with the MoFe-protein, Arg 100 (*109*) and Glu 112 (*110*),

are located on the same side of the protein as the 4Fe : 4S cluster. Hence, this surface almost certainly includes at least part of the interaction region between the two proteins. Relevant features of the interaction between Fe-protein and MoFe-protein that have been established biochemically include the ability of Glu 112 to crosslink with Lys β400 (*110*) and the likely occurrence of salt bridges in the interface region, as established by salt effects on nitrogenase activity (*111*) and the effects of replacing Arg 100 with other residues (*112*). As the Fe-protein dimer has a twofold symmetry axis, a plausible model (*16*) for docking the two proteins involves superposition of the Fe-protein twofold axis with the twofold axis passing through the P-cluster pair that relates the α and β subunits of the MoFe-protein (Fig. 8). The surfaces of the two proteins are complementary in this region; the MoFe-protein surface near the P-cluster pair has a convex shape, whereas the Fe-protein surface is concave about the 4Fe : 4S cluster. To either side of the P-cluster pair there are two wide and shallow clefts related by the pseudo-twofold axis that could accommodate the two Fe-protein subunits. With this orientation, the side chains of Glu 112 and Lys β400 can be positioned sufficiently close to permit crosslinking. Four short helices (α155–α159; α120–α125; β153–β158, and β120–β125), which are related by the pseudo-twofold axis, are oriented in parallel from the P-cluster pair toward the surface forming a four-helical bundle, and the 4Fe : 4S cluster of Fe-protein could bind to the top surface of these helices. The edge–edge distance from the P-cluster pair to the end of these helices is about 12 Å; thus the edge–edge distance from the P-cluster pair to the 4Fe : 4S cluster of Fe-protein may be about 15 Å. The consequences of site-directed mutations in or near these helices, at residues Phe β125 (*113*) and Asp α161 (D. Dean, personal communication), are consistent with a role for these residues in the MoFe-protein–Fe-protein interface. Additionally, substitutions of Glu α120 and Gly α160 in or near these helices have been identified in Nif$^-$ mutants, possibly due to disruption of the Fe-protein–MoFe-protein interaction (*101*). As the nucleotide binding site in this model for the complex is on the surface of the Fe-protein opposite to the interaction region with the MoFe-protein, it would seem possible for MgATP to exchange with MgADP without dissociation of the two proteins, as has been proposed from kinetic analyses of the nitrogenase reaction (*114*).

Kinetic studies indicate that nucleotide hydrolysis precedes electron transfer in the Fe-protein–MoFe-protein complex (*12, 13, 114*). Although the detailed structural consequences of nucleotide binding on the Fe-protein structure have not been established, it is likely that

MgATP hydrolysis is accompanied by a change in Fe-protein structure, such as an alteration in the relative orientations of the two subunits. Presumably, this transition leads to the formation of an activated species that is competent for electron transfer from the Fe-protein to the MoFe-protein (in particular, to the P-cluster pair in this model). A speculative model for the coupling of ATP hydrolysis to electron transfer involves the participation of residues ~62–70 of Fe-protein in the binding interaction with MoFe-protein (*15*). These residues, which exhibit a relatively large degree of sequence variability between different Fe-proteins, protrude from the same side of the Fe-protein surface as the cluster, Arg 100, and Glu 112. Residues 62–70 are part of a Fe-protein subdomain that encompasses residues 39–80. Changes upon binding to MoFe-protein in the position of this subdomain, relative to the remainder of Fe-protein, could be transmitted to Asp 39 or Asp 43, which are located within this region. Upon binding of Fe-protein to MoFe-protein, these residues, which are near the terminal phosphate groups of the nucleotide, could be repositioned to function as a general base catalyst in ATP hydrolysis. The coupling between nucleotide hydrolysis and conformational changes associated with intermolecular interactions is widespread in biochemistry and has been described for such diverse systems as the H-ras p21 oncogene protein (*115, 116*) and the rec A protein (*117*) that participates in DNA recombination.

Experimental studies have also indicated that oxidized MoFe-protein can bind MgADP (*68*), although it is not clear from the present studies where this site would be located and what the relationship of this site might be to the MoFe-protein metal centers and the proposed Fe-protein binding site. An alternative proposal for the structure of the complex would involve nucleotide binding at the interface between the Fe-protein and the MoFe-protein, with the active site for hydrolysis created by residues from both proteins. This type of interaction might be envisioned to involve the Fe-protein "opening" up along the subunit–subunit interface, which would expose the nucleotide binding sites, followed by contact between this region of the Fe-protein and the surface of the MoFe-protein above the P-cluster pair. Instead of the two proteins interacting in a "head-to-head" fashion, this would be more analogous to a "head-to-tail" binding interaction. The interface region of the Fe-protein would then involve residues at the bottom of the molecule, when viewed from the standard orientation (Fig. 4). Nif$^-$ mutations in this region of Fe-protein have been identified (*118*). Further genetic and structural studies of the MoFe-protein–Fe-protein complex will be of great interest to identify the mode(s) of interaction between these two proteins.

B. Role of the P-Cluster Pair

The presence of the disulfide bond in the P-cluster pair implies that this center can act as a two-electron redox group. One can imagine that two-electron chemistry can be driven by the cleavage and reformation of the μ_3-disulfide bridge, particularly since the disulfide is part of a metal cluster species common in electron transfer reactions. The role of the P-cluster pair could then be to mediate the electron transfer processes within the nitrogenase proteins by taking one-electron reducing equivalents provided by the Fe-protein and converting them into a two-electron transfer to the MoFe cofactor. This ability to exhibit both one- and two-electron redox chemistry would be analogous to the behavior of quinones and flavins in other biological systems.

A mechanism involving cleavage and reformation of a disulfide bond in the P-cluster pair may help explain the role of ATP in the flow of electrons through the nitrogenase system. If ATP hydrolysis were linked to a conformational change at the P-cluster pair that generated an activated state, this energy input could be utilized to generate more highly reduced electrons than are actually received from the Fe-protein. One way in which the energy released upon MgATP hydrolysis could be transduced into a lower potential superreducing P-cluster pair is illustrated by the following hypothetical mechanism (Fig. 9). Further reduction of a P-cluster pair having the structure exhibited in the dithionite reduced MoFe-protein would be difficult for two reasons: (i) all the iron sites appear to be in the Fe(II) state, as indicated by Mössbauer studies, and (ii) reduction of the disulfide bridge is unfavorable as the bridging cysteine ligands to the P-cluster pair constrain the two 4Fe : 4S clusters too closely (by ~1 Å) to accommodate nonbonded contacts between reduced sulfurs. The figure of ~1 Å is derived from the difference in the distance between the S—S bond length in a disulfide bridge (~2.1 Å) and the closest nonbonded distance between two sulfurs, which would be at least ~3 Å. This situation would change, however, if MgATP hydrolysis in the Fe-protein–MoFe-protein complex stabilized an altered conformation in which the bridging cysteine ligands were repositioned so that they no longer spanned the two 4Fe : 4S clusters. Since both the nucleotides and the P-cluster pair are at subunit interfaces, propagation of conformational changes from one site to the other would have precedence in the behavior of allosteric enzymes. The consequence of this hypothetical change in P-cluster pair ligation is that the reduction of the disulfide should now be sterically acceptable. Mechanistically, the problem would then be to reconcile the two-electron reduction of the disulfide with the one-electron redox

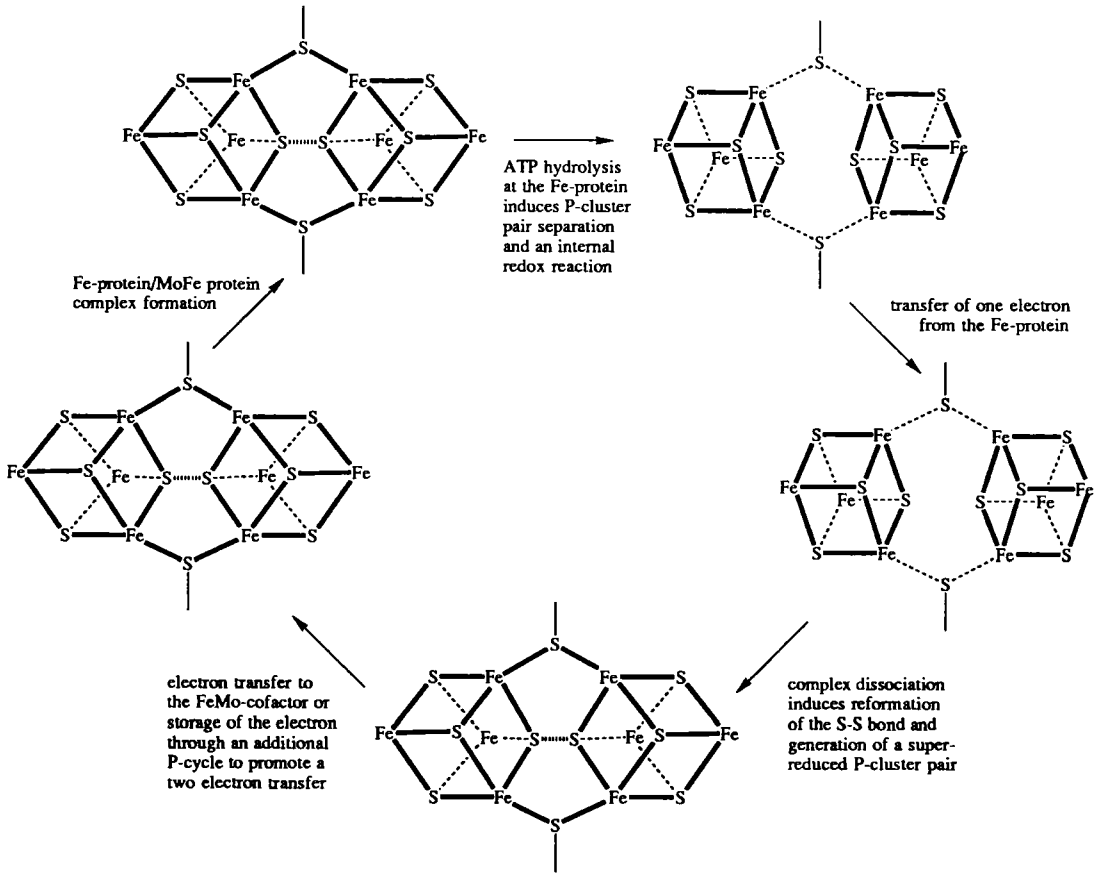

FIG. 9. A proposed P-cluster pair cycle (P-cycle) illustrating a possible sequence of electron transfer events at the P-cluster pair during substrate reduction by nitrogenase. See text for details.

properties of Fe-protein (although reports of the two-electron behavior of Fe-protein have appeared (*119*)). This could be achieved by a combination of an internal redox reaction in the P-cluster pair (corresponding formally to the oxidation of a single ferrous iron to ferric iron, accompanying the transfer of an electron to the disulfide bridge), along with the transfer of a single electron to the disulfide bridge from the Fe-protein. Alternatively, following the ATP-hydrolysis-induced conformational change, the disulfide bridge could be reduced by two electrons transferred internally from the P-cluster pair irons, with the Fe-protein electron formally transferred to the metal center.

Continuing with this hypothetical scenario, dissociation of the Fe-protein–MoFe-protein complex could follow reduction of the P-cluster pair. If complex dissociation (the rate-limiting step for the nitrogenase reaction) is accompanied by recoordination of the bridging cysteine ligands to the P-cluster pair, then a very unfavorable situation results with the reduced P-cluster pair constrained to adopt the geometry of the oxidized center. This form of the P-cluster pair would have a very low redox potential, and electron transfer from the P-cluster pair to the FeMo-cofactor would be thermodynamically facilitated, resulting in the production of superreducing electrons. Consequently, the role of MgATP hydrolysis in this scheme would be to generate a conformational state in which the P-cluster pair is more easily reduced, followed by dissociation of the protein–protein complex to generate low potential electrons. The P-cluster pair would then represent the site of energy transduction, at which the energy of ATP hydrolysis is captured as redox energy, much as the special bacteriochlorophyll dimer in photosynthetic reaction centers mediates the conversion of light to redox energy (*120*).

The possible existence of disulfide reduced forms of the P-cluster pair also suggests that hydrogen evolution could occur at this site. If upon conformationally induced separation of the reduced P-cluster pair, the inorganic sulfides became protonated, then reformation of the disulfide bond could result in formation of hydrogen. Hydrogen evolution by this mechanism at the P-cluster pair would also be consistent with the proposed mechanism of formation of the synthetic disulfide containing complex, $[Fe_4S_4(CO)_{12}]^{2-}$, which is thought to occur via the reaction of two $[(\mu\text{-S})(\mu\text{-HS})(Fe_2(CO)_6]^-$ intermediates to yield the product compound and hydrogen (*108*). It is also possible that a similar process leading to hydrogen evolution could be occurring in hydrogenases.

The preceding discussion has been based on the assumption that the P-cluster pair functions as an intermediate electron carrier between

the Fe-protein and the FeMo-cofactor. Assuming this is correct, the region between these two centers of the MoFe-protein would critically influence the mechanism and kinetics of intramolecular electron transfer. The edge–edge distance from the FeMo-cofactor to the P-cluster pair is about 14 Å. The homocitrate and Mo sites are on the side of the FeMo-cofactor that is closest to the P-cluster pair. Four α-helices (α63–α74; α88–α92; α191–α209, and β93–β106) are oriented in parallel between the two metal centers and may play an important role in electron transfer. In particular, the helices α63–α74 and α88–α92 adjacent to the P-cluster pair ligands Cys α62 and Cys α88 provide the most direct structural connection between the P-cluster pair and the FeMo-cofactor, and could perhaps participate in the formation of favorable electron transfer pathways (*121*) between the two centers. Additionally, potential proton transfer pathways, such as salt-bridge and hydrogen bonding networks, that could permit the coupling of electron and proton transfer between the P-cluster and the FeMo-cofactor have not been found, suggesting that these processes are not linked.

C. Substrate Binding to the FeMo-Cofactor

Great interest has been placed on understanding the structure and properties of the FeMo-cofactor as it is the most likely site of substrate reduction. Perhaps the key question to address is "What does the structure of the FeMo-cofactor suggest about the mechanism of dinitrogen reduction?" Unfortunately, crystallographic evidence concerning ligand binding to the FeMo-cofactor is not available and may never be available if only the more reduced forms of the cofactor generated during turnover can actually bind substrates (*122*). Despite (or because of) this lack of experimental information, some speculative aspects of the binding of substrates to the FeMo-cofactor may be formulated and are described below.

In attempting to deduce a mechanism for dinitrogen reduction, it is important to consider that the primary activation barrier arises in overcoming the kinetic stability of the dinitrogen triple bond. This suggests that binding modes that destabilize sp hybridized nitrogen or, alternatively, that stabilize sp^3 hybridized nitrogen would tend to activate dinitrogen for reduction. A large variety of possible binding geometries can be envisioned that involve binding of dinitrogen to one or more of the Fe, Mo, and/or S sites (*122a*). Rather than attempt to enumerate these possibilities, however, the discussion will instead be restricted to the possible binding of dinitrogen at the trigonally coordi-

nated iron sites of the FeMo-cofactor. It is tempting to imagine that the unusual unsaturated coordination of these irons could provide the site for substrate binding to the FeMo-cofactor.

The FeMo-cofactor appears to contain three-weak Fe—Fe bonds that would be further destabilized by the distortion from idealized tetrahedral geometry. Dinitrogen binding to the center of the FeMo-cofactor would replace these Fe—Fe bonds with multiple Fe—N bonds that would permit the iron atoms to adopt a less strained tetrahedral geometry (Fig. 10). Two formal resonance structures for this binding mode can be described: one in which the nitrogen atoms are triply bonded to each other and have only weak interactions with the irons, and a second in which the nitrogen atoms are formally sp^3 hybridized with a single bond between the nitrogens and to each of the irons. As a result of these multiple Fe—N interactions, the sp^3 form of nitrogen would be stabilized and the sp hybridized N≡N triple bond should be weakened, thereby lowering the activation barrier for dinitrogen reduction. Reduction of N_2 may be considered to be a shifting of the population of the dinitrogen bound resonance form to the hydrazine-like bound form. This model for N_2 reduction appears to provide a pathway by which large activation barriers are lowered for the most difficult step in the reduction of an N≡N triple bond to a single bond. Effectively, this model proposes that the FeMo-cofactor acts as host for a guest dinitrogen species, with the binding interactions occurring to facilitate activation for reduction.

Some precedence for the binding of nitrogen to trinuclear iron has been observed in the binding of diphenyldiazomethane to a trinuclear iron carbonyl cluster (*123*), but there is no precedence for *di*nitrogen binding in this fashion to well-characterized complexes. Indirect support for this binding interaction comes from a structure of C_2 with each carbon coordinated to a trinuclear arrangement of cobalts (*124*). What makes this acetylene-based structure particularly interesting is that the carbon–carbon bond distance indicates that the carbons exhibit

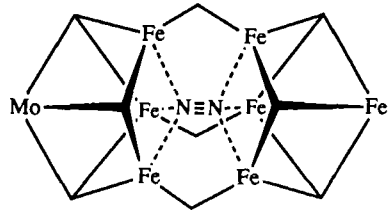

FIG. 10. A hypothetical model for the binding of dinitrogen to the FeMo-cofactor.

significant triple bonding interaction, despite their formal single bond coordination to six metal ions. Consequently, the C—C bond may be best described as a mixture of single and triple bonds, as proposed for the model for dinitrogen binding to the FeMo-cofactor.

Two potential problems with this model of dinitrogen binding to the FeMo-cofactor are recognized:

(1) In the dithionite reduced form of the MoFe-protein, the cavity size across the bridged irons inside the FeMo-cofactor structure is too small by ~0.5 Å to accommodate N_2. Consideration of the nitrogenase mechanism suggests that the more reduced forms of the cofactor actually bind N_2 (*122*), however, and it is possible that these more reduced forms have an increased separation distance between bridged Fe—Fe sites. S. Lippard (personal communication) has also suggested that protonation of the bridging sulfurs would also lead to an increased separation distance between Fe—Fe sites. By both mechanisms, expanded forms of the FeMo-cofactor that would permit N_2 binding could be generated. Consequently, in this "accordion" mechanism, the cavity inside the cofactor would expand and contract during the catalytic cycle to accommodate or expel substrates, intermediates, and products. As only N_2 is potentially small enough to coordinate inside the FeMo-cofactor, however, alternative binding modes would have to be available for utilization by different substrates, reaction intermediates, and inhibitors.

(2) It would be very difficult to protonate dinitrogen coordinated inside the FeMo-cofactor, particularly if protonation preceded electron transfer. If, however, following reduction, the N—N group rearranges to yield a species coordinated to only four Fe atoms, protons could in principle be added to these nitrogens on the exterior of the cofactor. The structure of a μ_4-peroxide tetrairon unit may be relevant to this binding mode (*125*). The immediate source of protons for transfer to bound intermediates could be from the hydrogen-bonding interactions displayed by the three bridging ligands of the cofactor. Further rearrangements are required to complete the steps in the proposed mechanism but similar rearrangements have been postulated for the reaction of azoalkane on a trinuclear center (*126*). Cleavage of the N—N bond and additional protonation reactions would yield the final product, ammonia.

In addition to the details of dinitrogen binding to the FeMo-cofactor, the number and sequence of electrons and protons transferred to the substrate is a critical question. Since all known substrates of nitrogenase are reduced by an even number of electrons, most mechanistic

speculation has focused on addition of (one or more) pairs of electrons to the substrate, leading formally to the reduction sequence: dinitrogen, diimide, hydrazine, and ammonia. The major activation barrier in this case would be the two-electron reduction of dinitrogen to diimide. One interesting possibility is that this barrier could be sidestepped by a four-electron reduction process, converting dinitrogen to the hydrazine oxidation level. This could be achieved by combination of a two-electron donation from the P-cluster pair, coupled with two electrons stored in the FeMo-cofactor, for example. Detailed mechanistic insight into nitrogenase can be achieved only by the development of experimental methods that can probe the fate of each electron transferred through the system.

VI. Future Outlook

One of the rationales for determining the structures of the nitrogenase proteins was to address the question "How does nitrogenase work?" Now that the structures are available, the same question is still just as relevant. Mechanistically, outstanding questions include details of the binding of substrates to the FeMo-cofactor (assuming that this does, indeed, take place); the number and types of intermediates in the reduction pathway and the mechanism by which they are formed; the pathway of electrons and protons through the nitrogenase system, including the role of the P-cluster pair; and the functional role of MgATP hydrolysis. The available experimental evidence permits the formulation of speculative answers to these questions, but more definitive answers remain elusive. Beyond the nitrogenase mechanism, important areas of research certainly include the synthesis and characterization of appropriate model compounds and details of the biological mechanism by which the active nitrogenase proteins are assembled. The assembly of such complex enzymatic machinery and the manner in which it might have arisen in the biological past are certainly fascinating problems.

Intriguing parallels may also exist between dinitrogen binding and activation by nitrogenase, and the industrial Haber–Bosch process. The Haber–Bosch process utilizes an iron catalyst to accelerate the rate of ammonia formation from dinitrogen and hydrogen. Various studies have demonstrated that the iron crystal surface with the highest catalytic activity is the Fe(111) plane (*127*). The iron sites on this surface are arranged with threefold symmetry, as are the bridging irons in the FeMo-cofactor. Additionally, Fe—Fe separations of ~2.5

and ~3.8 Å are observed in both types of catalysts. Significantly, binding of dinitrogen to the Fe(111) surface is accompanied by dissociation to atomic nitrogen, demonstrating that nitrogen–iron binding interactions can be sufficiently strong to weaken and/or break the nitrogen–nitrogen triple bond. It would indeed be ironic if it has taken ~80 years to recognize that an industrial process devised earlier this century actually mimics mechanistic features of the then undiscovered nitrogenase system.

ACKNOWLEDGMENTS

The contributions of M. Georgiadis, H. Komiya, D. Woo, B. T. Hsu, M. Day, G. Santillan, M. Stowell, J. Schlessman, and L. Joshua-Tor to this work are gratefully acknowledged, as are discussions with H. B. Gray and J. E. Bercaw. As always, the insights of J. B. Howard have been most illuminating. Structural studies of the MoFe-protein conducted by the author were supported by NSF CMB 91-18689, whereas the Fe-protein work was supported by NIH GM45162. M. K. Chan was supported by NIH Fellowship 1F32 GM15006.

REFERENCES

1. Olivé, G. H., and Olivé, S., *in* "A Treatise on Dinitrogen Fixation" R. W. F. Hardy, F. Bottomley, and R. C. Burns, eds.), p. 3. Wiley, New York, 1979.
2. Burgess, B. K., *in* "Advances in Nitrogen Fixation" (C. Veeger, and W. E. Newton, eds.), p. 103. Martinus Nijhoff, Boston, 1984.
3. Orme-Johnson, W. H., *Annu. Rev. Biophys. Biophys. Chem.* **14,** 419 (1985).
4. Holm, R. H., and Simhon, E. D., *in* "Molybdenum Enzymes" T. G. Spiro, ed.), Chapter 1. Wiley (Interscience); New York, 1985.
5. Stiefel, E. I., Thomann, H., Jin, H., Bare, R. E., Morgan, T. V., Burgmayer, S. J. N., and Coyle, C. L., *in* "Metal Clusters in Proteins" (L. Que, ed.), p. 372. Am. Chem. Soc., Washington, DC, 1988.
6. Burris, R. H., *J. Biol. Chem.* **266,** 9339 (1991).
7. Smith, B. E., and Eady, R. R., *Eur. J. Biochem.* **205,** 1 (1992).
8. Stacey, G., Burris, R. H., and Evans, H. J., eds., "Biological Nitrogen Fixation." Chapman & Hall, New York, 1992.
9. Eady, R. R., *Adv. Inorg. Chem.* **36,** 77 (1991).
10. Bishop, P. E., and Premakuman, R., *in* "Biological Nitrogen Fixation" (G. Stacey, R. H. Burris, and H. J. Evans, eds.), p. 736. Chapman & Hall, New York, 1992.
11. Simpson, F. B., and Burris, R. H., *Science* **224,** 1095 (1984).
12. Lowe, D. J., and Thorneley, R. N. F., *Biochem. J.* **215,** 393 (1983).
13. Lowe, D. J., and Thorneley, R. N. F., *Biochem. J.* **224,** 895 (1984).
14. Hageman, R. V., and Burris, R. H., *Biochemistry* **17,** 4117 (1978).
15. Georgiadis, M. M., Komiya, H., Chakrabarti, P., Woo, D., Kornuc, J. J., and Rees, D. C., *Science* **257,** 1653 (1992).

16. Kim, J., and Rees, D. C. *Science* **257,** 1677 (1992).
17. Kim, J., and Rees, D. C., *Nature (London)* **360,** 553 (1992).
18. Chan, M. K., Kim, J., and Rees, D. C., *Science* **260,** 792 (1993).
19. Kim, J., Woo, D., and Rees, D. C., *Biochemistry* **32,** 7104 (1993).
19a. Bolin, J. T., Campobasso, N., Muchmore, S. W., Minor, W., Morgan, T. V., Mortenson, L. E., *in* "New Horizons in Nitrogen Fixation" (R. Palacios, J. Mora, and W. E. Newton, eds.) p. 89. Kluwer, Dordrecht, 1993.
20. Normand, P., and Bousquet, J., *J. Mol. Evol.* **29,** 436 (1989).
21. Hausinger, R. P., and Howard, J. B., *J. Biol. Chem.* **257,** 2483 (1989).
22. Tanaka, M., Haniu, M., Yasunobu, K. T., and Mortenson, L. E., *J. Biol. Chem.* **252,** 7081 (1977).
23. Hausinger, R. P., and Howard, J. B., *J. Biol. Chem.* **258,** 13486 (1983).
24. Howard, J. B., Davis, R., Moldenhauer, B., Cash, V. L., and Dean, D., *J. Biol. Chem.* **264,** 11270 (1989).
25. Lindahl, P. A., Day, E. P., Kent, T. A., Orme-Johnson, W. H., and Münck, E., *J. Biol. Chem.* **260,** 11160 (1985).
26. Hagen, W. R., Eady, R. R., Dunham, W. R., and Haaker, H., *FEBS Lett.* **189,** 250 (1985).
27. Watt, G. D. and McDonald, D. W. *Biochemistry* **24,** 7226 (1985).
28. Morgan, T. V., Prince, R. C., and Mortenson, L. E., *FEBS Lett.* **206,** 4 (1986).
29. Yates, M. G., *in* "Biological Nitrogen Fixation" (G. Stacey, R. H. Burris, and H. J. Evans, eds.), p. 685. Chapman & Hall, New York, 1992.
30. Watt, G. D., Wang, Z.-C., and Knotts, R. R., *Biochemistry* **25,** 8156 (1986).
31. Zumft, W., Mortenson, L., and Palmer, G., *Biochim. Biophys. Acta* **292,** 413 (1973).
32. Walker, G. A., and Mortenson, L. E., *Biochem. Biophys. Res. Commun.* **53,** 904 (1973).
33. Walker, G. A., and Mortenson, L. E., *Biochemistry* **13,** 2382 (1974).
34. Ljones, T., and Burris, R. H., *Biochemistry* **17,** 1866 (1978).
35. Anderson, G. L., and Howard, J. B., *Biochemistry* **23,** 2118 (1984).
36. Deits, T. L., and Howard, J. B., *J. Biol. Chem.* **264,** 6619 (1989).
37. Wolle, D., Dean, D. R., and Howard, J. B., *Science* **258,** 992 (1992).
38. Gavini, N., and Burgess, B. K., *J. Biol. Chem.* **267,** 21179 (1992).
39. Seefeldt, L. C., Morgan, T. V., Dean, D. R., and Mortenson, L. E., *J. Biol. Chem.* **267,** 6680 (1992).
40. Robinson, A. C., Dean, D. R., and Burgess, B. K., *J. Biol. Chem.* **262,** 14327 (1987).
41. Robinson, A. C., Chu, W., Li, J.-G., and Burgess, B. K., *J. Biol. Chem.* **264,** 10088 (1989).
42. Tal, S., Chun, T. W., Gavini, N., and Burgess, B. K., *J. Biol. Chem.* **266,** 10654 (1991).
43. Joerger, R. D., Wolfinger, E. D., and Bishop, P. E., *J. Bacteriol.* **173,** 4440 (1991).
44. Howard, K. S., McLean, P. A., Hansen, F. B., Lemley, P. V., Koblan, K. S., and Orme-Johnson, W. H., *J. Biol. Chem.* **261,** 772 (1986).
45. Paul, W., and Merrick, M., *Eur. J. Biochem.* **178,** 675 (1989).
46. Brigle, K. E., Newton, W. E., and Dean, D. R., *Gene* **37,** 37 (1985).
47. Wang, S.-Z, Chen, J.-S., and Johnson, J. L., *Biochemistry* **27,** 2800 (1988).
48. Burgess, B. K., *Chem. Rev.* **90,** 1377 (1990).
49. Newton, W. E., *in* "Biological Nitrogen Fixation" (G. Stacey, R. H. Burris, and H. J. Evans, eds.), p. 877. Chapman & Hall, New York, 1992.
50. Shah, V. K., and Brill, W. J., *Proc. Natl. Acad. Sci. U.S.A.* **74,** 3249 (1977).
51. Hawkes, T. R., McLean, P. A., and Smith, B. E., *Biochem. J.* **217,** 317 (1984).
52. Imperial, J., Hoover, T. R., Madden, M. S., Ludden, P. W., and Shah, V. K., *Biochemistry* **28,** 7796 (1989).

53. Nelson, M. J., Levy, M. A., and Orme-Johnson, W. H., *Proc. Natl. Acad. Sci. U.S.A.* **80,** 147 (1983).
54. Hoover, T. R., Robertson, A. D., Cerny, R. L., Hayes, R. N., Imperial, J., Shah, V. K., and Ludden, P. W., *Nature (London)* **329,** 855 (1987).
55. Madden, M. S., Kindon, N. D., Ludden, P. W., and Shah, V. K., *Proc. Natl. Acad. Sci. U.S.A.* **87,** 6517 (1990).
56. Holm, R. H., Ciurli, S., and Weigel, J. A., *Prog. Inorg. Chem.* **38,** 1 (1990).
57. Smith, B. E., and Lang, G., *Biochem. J.* **137,** 169 (1974).
58. Kurtz, D. M., McMillan, R. S., Burgess, B. K., Mortenson, L. E., and Holm, R. H., *Proc. Natl. Acad. Sci. U.S.A.* **76,** 4986 (1979).
59. Zimmermann, R., Münck, E., Brill, W. J., Shah, V. K., Henzl, M. T., Rawlings, J., and Orme-Johnson, W. H., *Biochim. Biophys. Acta* **537,** 185 (1978).
60. Huynh, B. H., Henzl, M. T., Christner, J. A., Zimmermann, R., Orme-Johnson, W. H., and Münck, E., *Biochim. Biophys. Acta* **623,** 124 (1980).
61. McLean, P. A., Papaefthymiou, V., Orme-Johnson, W. H., and Münck, E., *J. Biol. Chem.* **262,** 12900 (1987).
62. Lindahl, P. A., Papaefthymiou, V., Orme-Johnson, W. H., and Münck, E., *J. Biol. Chem.* **263,** 19412 (1988).
63. Hagen, W. R., Wassink, H., Eady, R. R., Smith, B. E., and Haaker, H., *Eur. J. Biochem.* **169,** 457 (1987).
64. Surerus, K. K., Hendrich, M. P., Christie, P. D., Rottgardt, D., Orme-Johnson, W. H., and Münck, E., *J. Am. Chem. Soc.* **114,** 8579 (1992).
65. Pierik, A. J., Wassink, H., Haaker, H., and Hagen, W. R., *Eur. J. Biochem.* **212,** 51 (1993).
66. Bolin, J. T., Ronco, A. E., Mortenson, L. E., Morgan, T. V., Williamson, M., and Xuong, N.-H., *in* "Nitrogen Fixation: Achievements and Objectives" (P. M. Gresshoff, L. E. Roth, G. Stacey, and W. E. Newton, eds.), p. 117. Chapman & Hall; New York, 1990.
67. Tittsworth, R., and Hales, B. J., *Int. Congr. Nitrogen Fixation, 9th,* Cancún, Mexico, *1992,* Abstr. 307 (1992).
68. Miller, R. W., and Eady, R. R., *Biochem. J.* **263,** 725 (1989).
69. Peterson, J., Fisher, and K., Lowe, D. J., *Int. Congr. Nitrogen Fixation, 9th,* Cancún, Mexico, *1992,* Abstr. 306 (1992).
70. Björkman, P. J., Saper, M. A., Samraoui, B., Bennett, W. S., Strominger, J. L., and Wiley, D. C., *Nature (London)* **329,** 506 (1987).
71. Herkovitz, T., Averill, B. A., Holm, R. H. Ibers, J. A., Phillips, W. D., Weiher, J. F., *Proc. Natl. Acad. Sci. U.S.A.* **69,** 2437 (1972).
72. Coucouvanis, D., *Acc. Chem. Res.* **24,** 1 (1991).
73. Kent, H. K., Ioannidis, I., Gormal, C., Smith, B. E., and Buck, M., *Biochem. J.* **264,** 257 (1989).
74. Kent, H. M., Baines, M., Gormal, C., Smith, B. E., and Buck, M., *Mol. Microbiol.* **4,** 1497 (1990).
75. Scott, D. J., May, H. D., Newton, W. E., Brigle, K. E., and Dean, D. R., *Nature (London)* **343,** 188 (1990).
76. Dean, D. R., Setterquist, R. A., Brigle, K. E., Scott, D. J., Laird, N. F., and Newton, W. E., *Mol. Microbiol.* **4,** 1505 (1990).
77. May, H. D., Dean, D. R., and Newton, W. E., *Biochem. J.* **277,** 457 (1991).
78. Thomann, H., Morgan, T. V., Jin, H., Burgmayer, S. J. N., Bare, R. E., and Stiefel, E. I., *J. Am. Chem. Soc.* **109,** 7913 (1987).
79. Thomann, H., Bernardo, M., Newton, W. E., and Dean, D. R., *Proc. Natl. Acad. Sci. U.S.A.* **88,** 6620 (1991).

80. Howard, J. B., and Rees, D. C., *Adv. Protein Chem.* **42,** 199 (1991).
81. Carson, M., and Bugg, C. E., *J. Mol. Graphics* **4,** 121 (1986).
82. Walker, J. E., Saraste, M., Runswick, M. J., and Gay, N. J., *EMBO J.* **8,** 945 (1982).
83. Schulz, G. E., *Curr. Opin. Struct. Biol.* **2,** 61 (1992).
84. Robson, R. J., *FEBS Lett.* **173,** 394 (1984).
85. Morgan, T. V., McCracken, J., Orme-Johnson, W. H., Mims, W. B., Mortenson, L., and Peisach, J., *Biochemistry* **29,** 3077 (1989).
86. Lindahl, P. A., Gorelick, N. J., Münck, E., and Orme-Johnson, W. H., *J. Biol. Chem.* **262,** 14945 (1987).
87. Fujita, Y., Takahashi, Y., Kohchi, T., Ozeki, H., Ohyama, K., and Matsubara, H., *Plant Mol. Biol.* **13,** 551 (1989).
88. Burke, D. H., Alberti, M., Hearst, J., *J. Bacteriol.* **175,** 2407 (1993).
89. Karkaria, C. E., Chen, C. M., and Rosen, B. P., *J. Biol. Chem.* **265,** 7832 (1990).
90. Lammers, P. J., and Haselkorn, R., *Proc. Natl. Acad. Sci. U.S.A.* **80,** 4723 (1983).
91. Bhat, T. N., Blow, D. M., Brick, P., and Nyborg, J., *J. Mol. Biol.* **158,** 699 (1982).
92. Robbins, A. H., and Stout, C. D., *Proteins: Struct. Funct., Genet.* **5,** 289 (1989).
93. Meyer, J., Gaillard, J., and Moulis, J.-M., *Biochemistry* **27,** 6150 (1988).
94. Deisenhofer, J., Epp, O., Miki, K., Huber, R., and Michel, H., *Nature (London)* **318,** 618 (1985).
95. Allen, J. P., Feher, G., Yeates, T. O., Komiya, H., and Rees, D. C., *Proc. Natl. Acad. Sci. U.S.A.* **84,** 5730 (1987).
96. Godden, J. W., Turley, S., Teller, D. C., Adman, E. T., Liu, M. Y., Payne, W. J., and LeGall, J., *Science* **253,** 438 (1991).
97. Morgan, T. V., McCracken, J., Orme-Johnson, W. H., Mims, W. B., Mortenson, L., and Peisach, J., *Biochemistry* **29,** 3077 (1990).
98. Adman, E. T., Watenpaugh, K. D., and Jensen, L. H., *Proc. Natl. Acad. Sci. U.S.A.* **72,** 4854 (1975).
99. Johansson, G., and Lipscomb, W. N., *Acta Crystallogr.* **11,** 594 (1958).
100. Chu, C. T.-W., and Dahl, L. F., *Inorg. Chem.* **16,** 3245 (1977).
101. Govenzensky, D., and Zamir, A., *J. Bacteriol.* **171,** 5729 (1989).
102. Scott, D. J., Dean, D. R., and Newton, W. E., *in* "Nitrogen Fixation: Achievements and Objectives" (P. M. Gresshoff, L. E. Roth, G. Stacey, and W. E. Newton, eds.), p. 169. Chapman & Hall, New York, 1990.
103. Power, P. P., and Shoner, S. C., *Angew. Chem., Int. Ed. Engl.* **30,** 330 (1991).
104. Eidsness, M. K., Flank, A. M., Smith, B. E., Flood, A. C., Garner, C. D., and Cramer, S. P., *J. Am. Chem. Soc.* **108,** 2746 (1986).
105. Conradson, S. D., Burgess, B. K., Newton, W. E., Mortenson, L. E., and Hodgson, K. O., *J. Am. Chem. Soc.* **109,** 7507 (1987).
106. Arber, J. M., Flood, A. C., Garner, C. D., Gormal, C. A., Hasnain, S., and Smith, B. E., *Biochem. J.* **252,** 421 (1988).
107. True, A. E., Nelson, M. J., Venters, R. A., Orme-Johnson, W. H., Hoffman, B. M., *J. Am. Chem. Soc.* **110,** 1935 (1988).
108. Bose, K. S., Sinn, E., and Averill, B. A., *Organometallics* **3,** 1126 (1984).
109. Murrell, S. A., Lowery, R. G., and Ludden, P. W., *Biochem. J.* **251,** 609 (1988).
110. Willing, A., and Howard, J. B., *J. Biol. Chem.* **265,** 6596 (1990).
111. Deits, T. L., and Howard, J. B., *J. Biol. Chem.* **265,** 3859 (1990).
112. Wolle, D., Kim, C.-H., Dean, D., and Howard, J. B., *J. Biol. Chem.* **267,** 3667 (1992).
113. Thorneley, R. N. F., Ashby, G. A., Fisher, K., and Lowe, D. J., *in* "Molybdenum Enzymes, Cofactors and Models" (E. Stiefel, D. Coucouvanis, and W. E. Newton, eds.). Am. Chem. Soc., Washington, DC, 1993 (in press).

114. Thorneley, R. N. F., *in* "Nitrogen Fixation: Achievements and Objectives" (P. M. Gresshoff, L. E. Roth, G. Stacey, and W. E. Newton, eds.), p. 103. Chapman & Hall, New York, 1990.
115. Brünger, A. T., Milburn, M. V., Tong, L., DeVos, A. M., Jancarik, J., Yamaizumi, A., Nishimura, S., Ohtsuka, E., and Kim, S. H., *Proc. Natl. Acad. Sci. U.S.A.* **87,** 4849 (1990).
116. Pai, E. F., Krengel, U., Petsko, G. A., Goody, R. S., Kabsch, W., and Wittinghofer, A., *EMBO J.* **9,** 2351 (1990).
117. Story, R. M., and Steitz, R. A., *Nature (London)* **355,** 374 (1992).
118. Bagiunon, M. C., Smith, X. G., and Davis, L. C., *Int. Cong. Nitrogen Fixation, 9th,* Cancún, Mexico, *1992,* Abstr. 317 (1992).
119. Watt, G. D., *204th Am. Chem. Soc. Nat. Meet.,* Washington, D.C., *1992,* Abstr. INOR-143 (1992).
120. Feher, G., Allen, J. P., Okamura, M. Y., and Rees, D. C., *Nature (London)* **339,** 111 (1989).
121. Wuttke, D. S., Bjerrum, M. J., Winkler, J. R., and Gray, H. B., *Science* **256,** 1007 (1992).
122. Thorneley, R. N. F., and Lowe, D. J., in "Molybdenum Enzymes" (T. Spiro, ed.), p. 221. Wiley (Interscience) New York, 1985.
122a. Deng, H., and Hoffmann, R., *Angew. Chem. Int. Ed.* (in press).
123. Baikie, P. E., and Mills, O. S., *Chem. Commun.* p. 1228 (1967).
124. Brice, M. D., and Penfold, B. R., *Inorg. Chem.* **11,** 1381 (1972).
125. Micklitz, W., Bott, S. G., Bensten, J. G., and Lippard, S. J., *J. Am. Chem. Soc.* **111,** 372 (1989).
126. Wucherer, E. J., Tasi, M., Hansert, B., Powell, A. K., Garland, M.-T., Halet, J.-F., Saillard, J.-Y., and Vahrenkamp, H., *Inorg. Chem.* **28,** 3564 (1989).
127. Jennings, J. R., ed., "Catalytic Ammonia Synthesis: Fundamentals and Practice." Plenum, New York, 1991.